Proceedings of the 29th Chinese Control Conference
July 29-31, 2010, Beijing, China

Adaptive Control and Optimal Power/Brake Distribution of High Speed Trains with Uncertain Nonlinear Couplers*

SONG Qi[1], SONG Yongduan[1,2]
[1]Center for Intelligent Systems and Renewable Energy, Beijing Jiaotong University, Beijing 100044, P.R.China.
[2]State Key Laboratory of Rail Traffic Control and Safety, Beijing Jiaotong University, Beijing 100044, P.R.China.
E-mail: songyd_ncat@yahoo.com

Abstract: This paper focuses on the position and velocity tracking control problem of high speed trains consisting of multiple vehicles (i.e., locomotives and carriages). A new dynamic model explicitly reflecting the interactive impacts among the vehicles is established using multiple point-mass Newton equations. Such impacts, together with aerodynamic resistance, mechanical resistance and some other additional resistances due to uncertain operation railway conditions, are addressed in control design. Robust adaptive control strategy is proposed to ensure high precision speed and position tracking, which is realized through optimal power and brake distribution among the vehicles. It is shown that the control scheme is not only robust against external disturbances, but also adaptive to unknown system parameters. The effectiveness of the proposed approach is also confirmed through numerical simulations.

Key Words: Multiple Point-Mass Model, In-Train Force, Robust Adaptive Control, High Speed Train, Optimal Power/Brake Distribution

1 INTRODUCTION

Since the aerodynamic drag is proportional to the square of the speed at which the train travels, its influence on train dynamic behavior becomes increasingly significant as the train speed increases. This fact, together with the additional interactive impacts from the vehicles connected through couplers, makes the train speed and position tracking control problem interesting yet challenging, which has enticed considerable attention from researchers in control community [6~11].

Most existing works are either based upon single point-mass model [1~5] or multiple point-mass model [6~11]. Because of its simplicity, single point-mass model has been widely used, which treats the train consisting of multiple vehicles as a single rigid body and characterizes the longitudinal motion of the train approximately by a single point-mass Newtown equation [1-5].

However, as the couplers connecting adjacent vehicles are not perfectly rigid, the impacts from the connected vehicles have to be explicitly considered in order to achieve satisfactory control performance. Several researchers have tackled various control issues of cargo or passenger trains in the past few years, where multiple point-mass model containing in-train force impact between neighboring vehicles is explicitly utilized [9-11].

On the other hand, while multiple point-mass model is more effective in characterizing the dynamic behavior of the train, control design and stability analysis based on such model become much more involved unless it is linearized along a prior scheduled ideal speed [10,11]. Furthermore, since the number of passengers/loads on board each vehicle is different and uncertain in general, the total mass of each vehicle is unavailable for control design, thus a new control method that is independent of such mass parameter as well as other resistive coefficients is highly desirable.

The purpose of this paper is to address the speed and position tracking control problem based on the nonlinear and elastic nature of the impacts among the locomotives and carriages. A new dynamic model that reflects vehicle coupling effects (called in-train forces in the literature [9]) is established. As the in-train forces are difficult to measure and control directly, a single (unified) coordinate system is employed in describing the displacement and velocity of the train systems, which renders the multiple dimensional model into a single dimensional model in which the in-train forces are naturally cancelled out. Robust adaptive control strategy is developed to ensure high precision speed and position tracking via optimal power and brake distribution among the vehicles. It is shown that the control scheme is not only robust against external disturbances, but also adaptive to unknown system parameters. The effectiveness of the proposed approach is also confirmed through numerical simulations.

2 MULTIPLE POINT-MASS MODEL

Consider a train system with n carriages, as shown in Fig. 1. Assume that the carriages are linked with connections which might be elastic as illustrated in Fig. 2.

Let x_i denote the distance between the center of the ith vehicle and the reference point, $\Delta x_i = \vartheta_i + \Delta x_{di}$ denote the length of the link between the ith carriage and the $(i+1)$th one, where ϑ_i is a constant corresponding to the original length of the link without any elastic deformation; Δx_{di} represents the extension or compression of the ith spring connector, which could be positive or negative. It is then readily obtained that the distance between the ith vehicle

*This work was supported in part by National Natural Science Foundation of China under the grant No. 60974052.

and the $(i+1)$th vehicle can be written as $x_{i+1}-x_i = d_i + \Delta x_i + d_{i+1}$, where d_i is positive constant with the physical meaning as shown in Fig. 2.

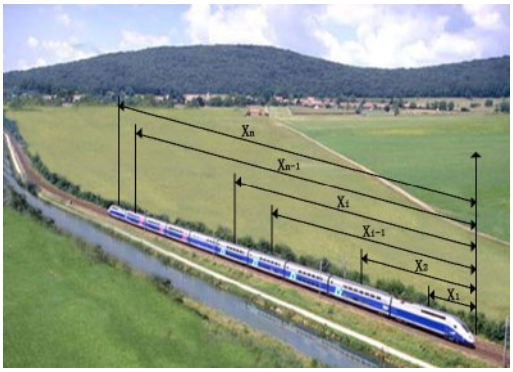

Fig. 1 Train with multiple carriages

Obviously, considering all the vehicles connected one can establish the following, for $i = 1, 2, ..., n$

$$x_i - x_{i-1} = d_{i-1} + \Delta x_{i-1} + d_i$$

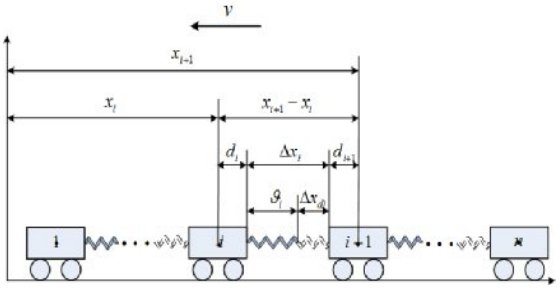

Fig. 2 Carriages with elastic connections

In light of $\Delta x_i = \vartheta_i + \Delta x_{di}$, it follows that

$$\dot{x}_i = \dot{x}_{i-1} + \Delta\dot{x}_{d(i-1)}$$

and

$$\ddot{x}_i = \ddot{x}_{i-1} + \Delta\ddot{x}_{d(i-1)}$$

which can be written uniformly as

$$\begin{aligned} \dot{x}_i &= \dot{x}_1 + \sum_{j=1}^{i-1} \Delta\dot{x}_{dj} \quad (i = 2,3,\cdots,n) \\ \ddot{x}_i &= \ddot{x}_1 + \sum_{j=1}^{i-1} \Delta\ddot{x}_{dj} \quad (i = 2,3,\cdots,n) \end{aligned} \tag{1}$$

By Newton's law, the dynamic motion equation for each vehicle can be established as follows,

$$\begin{cases} m_1\ddot{x}_1 = \lambda_1 F_1 - f_{d1} + f_{in_0} - f_{in_1} \\ m_2\ddot{x}_2 = \lambda_2 F_2 - f_{d2} + f_{in_1} - f_{in_2} \\ \vdots \\ m_i\ddot{x}_i = \lambda_i F_i - f_{di} + f_{in_{(i-1)}} - f_{in_i} \\ \vdots \\ m_n\ddot{x}_n = \lambda_n F_n - f_{dn} + f_{in_{(n-1)}} - f_{in_n} \end{cases} \tag{2}$$

where m_i is the mass of the ith vehicle, x_i is defined as before; λ_i is a distribution constant determining the power/braking effort of the ith vehicle; F_i and f_{di} denote the traction/braking force and the resistance on the ith vehicle, respectively. f_{di} consists of mechanical resistance which is proportional to the train speed (described as $a_0 + a_1\dot{x}_i$, where a_0 and a_1 are the mechanical resistance coefficients respectively), aerodynamic resistance which is proportional to the square of the speed (known as $a_2\dot{x}_i^2$, where a_2 is the aerodynamic resistance coefficient) , ramp resistance (f_{ri}) due to the track slope, curve resistance (f_{ci}) due to railway curvature, and tunnel resistance (f_{ti}), *et*c.. Namely, f_{di} can be described as

$$f_{di} = a_0 + a_1\dot{x}_i + a_2\dot{x}_i^2 + f_{ri} + f_{ci} + f_{ti} \tag{3}$$

The variables a_0 , a_1 and a_2 depend on factors such as vehicle type, structure, weather condition, wind speed, wind direction, etc. [13~15]. Apparently, those coefficients are difficult to obtain precisely in practice. Note that f_{in_i} is the force from the couplers connecting the adjacent vehicles (called in-train force as in [10,11] hereafter) and obviously $f_{in_0} = 0$ and $f_{in_n} = 0$ because no such in-train force exists for the first and the last vehicle.

If treating the carriage individually, one would have to deal with *multiple* dimensional dynamic equations with n different coordinates. If, however, the relation (1) is used one can express (2) in terms of a single coordinate, i.e., x_1 only (or any one of the coordinate) as follows,

$$\begin{cases} m_1\ddot{x}_1 = \lambda_1 F_1 - f_{d1} + f_{in_0} - f_{in_1} \\ m_2\ddot{x}_1 = \lambda_2 F_2 - f_{d2} + f_{in_1} - f_{in_2} - m_2\Delta\ddot{x}_{d1} \\ \vdots \\ m_i\ddot{x}_1 = \lambda_i F_i - f_{di} + f_{in_{(i-1)}} - f_{in_i} - m_i\sum_{j=1}^{i-1}\Delta\ddot{x}_{dj} \\ \vdots \\ m_n\ddot{x}_1 = \lambda_n F_n - f_{dn} + f_{in_{(n-1)}} - f_{in_n} - m_n\sum_{j=1}^{n-1}\Delta\ddot{x}_{dj} \end{cases}$$

Remark 1 In the literature, the in-train force is either modeled as a linear spring and damper [10,11] or softening/hardening spring [6,7]. In general, however, it is difficult to model or measure such in-train force precisely due to the nonlinear and elastic nature of the couplers.

To circumvent this difficulty, an alternative approach is used to deal with such in-train forces. First, observe that the in-train forces f_{in_i} always appear in opposite direction between any two vehicles regardless of the connection being rigid or flexible. This motivates the use of summation of the above equations to get

$$\begin{aligned} &(m_1 + m_2 + \cdots + m_n)\ddot{x}_1 \\ &= (\lambda_1 \quad \lambda_2 \quad \cdots \quad \lambda_n)\begin{pmatrix} F_1 \\ F_2 \\ \vdots \\ F_n \end{pmatrix} - \sum_{i=1}^{n} f_{di} \\ &\quad - \Delta\ddot{x}_{d1}\sum_{i=2}^{n} m_i - \Delta\ddot{x}_{d2}\sum_{i=3}^{n} m_i \\ &\quad - \cdots - \Delta\ddot{x}_{d(n-1)} m_n \end{aligned}$$

As a result, the in-train forces are cancelled out naturally. Expressed compactly, one has

$$M(m_i)\ddot{x}_1 = \begin{pmatrix}\lambda_1 & \lambda_2 & \cdots & \lambda_n\end{pmatrix}\begin{pmatrix}F_1\\F_2\\\vdots\\F_n\end{pmatrix} + F_d(\cdot) \tag{4}$$

where $M(m_i) = \sum_{i=1}^{n} m_i$,

$$\begin{aligned} F_d(\cdot) = &-\sum_{i=1}^{n} f_{di} - \Delta\ddot{x}_{d1}\sum_{i=2}^{n} m_i \\ &- \Delta\ddot{x}_{d2}\sum_{i=3}^{n} m_i - \cdots - \Delta\ddot{x}_{d(n-1)}m_n \end{aligned} \tag{5}$$

Remark 2 The resultant model is a multiple point-mass single coordinate model. The existing single point-mass model used in most previous works can be viewed as a special case of the one presented here. It is important to note that when multiple point-mass model is considered, additional external resistive forces are present in the model, which are usually overlooked in most existing works. The total aerodynamic drag comes from all the vehicles and each contributes to such drag differently. Therefore, it seems that the model presented here is more appropriate to characterize the dynamic behaviors of high speed train with multiple carriages.

3 CONTROL AND POWER DISTRIBUTION

For simple notation, (4) is rewritten as

$$M\dot{v} = \Lambda F + F_d \tag{6}$$

with F_d is defined as in (5), M is the total mass of the train, which might not be accurately available due to uncertain variation of passengers and loads, since the number of passengers on board each vehicle is different and uncertain in general, the total mass of each vehicle is uncertain. $\Lambda = [\lambda_1,...,\lambda_n]$ is the power distribution matrix, $x = x_1$ is the position of the first vehicle with respect to the reference point, $F \in R^n$ denotes the control force vector (traction or braking force), F_d is the term containing various resistive forces and the impacts among the vehicles.

Remark 3 Note that while $\Delta\dot{x}_{di}$ and $\Delta\ddot{x}_{di}$ could be physically obtained from $\dot{x}_{i+1} - \dot{x}_i = \Delta\dot{x}_{di}$ and $\ddot{x}_{i+1} - \ddot{x}_i = \Delta\ddot{x}_{di}$ respectively, it would require a total number of n sensors for speed measurement and n sensors for acceleration measurement, which is too costly. If only x_1 and $\dot{x}_1$ are available, as assumed in this study, then $\Delta\dot{x}_{di}$ and $\Delta\ddot{x}_{di}$ are unknown and immeasurable, thus their impacts on the train dynamic behaviors are also unpredictable. However, it is reasonable to assume that, unless there is sudden change of speed due to emergency, the impacts of $\Delta\dot{x}_{di}$ and $\Delta\ddot{x}_{di}$ are limited in that $|\Delta\dot{x}_{di}| \leqslant c_{1i} < \infty$ and $|\Delta\ddot{x}_{di}| \leqslant c_{2i} < \infty$, where c_{1i} and c_{2i} are constants.

3.1 Problem Formulation

To facilitate the control design, we define a filtered variable

$$s = \dot{e} + \beta e \tag{7}$$

where β is a free positive parameter chosen by the designer/user, and x and x^* denote the actual train position and the desired train position respectively. $e = x - x^*$ denotes the position tracking error, and $\dot{e} = \dot{x} - \dot{x}^*$ is the velocity tracking error. From (6) and (7), it is straightforward to show that:

$$M\dot{s} = \Lambda F - M(\ddot{x}^* - \beta\dot{e}) + F_d(\cdot) \tag{8}$$

$F_d(\cdot)$ is as defined in (5). With the assumption that $\Delta\dot{x}_{di}$, $\Delta\ddot{x}_{di}$, and m_i are bounded, it is established that

$$|F_d| \leqslant b_1 + b_2|\dot{x}| + b_3|\dot{x}|^2 \leqslant b\Phi \tag{9}$$

$$\Phi = 1 + |\dot{x}| + |\dot{x}|^2 \tag{10}$$

where b_1, b_2, and b_3 are some non-negative constants, and $b = \max\{b_1, b_2, b_3\}$. It is important to note that both Eqs. (9) and (10) are true regardless of external disturbances, uncertain train mass, or type of vehicle. Moreover, it is worth noting that the precise analytical estimate of the upper bound coefficient b is a painful task in control design, and the mass of the train M is difficult to obtain precisely too, thus it is highly desirable to develop a control scheme that does not rely on any such coefficients.

3.2 Robust Adaptive Control Design

The control objective is to design control force F so that for any given desired $\dot{x}^* - x^*$ pair or $x^* - t$ and $v^* - t$, it is ensured that $e \to 0$, $\dot{e} \to 0$ as $t \to \infty$. F is traction force when $F > 0$, braking force when $F < 0$. When F is zero, the train is in free motion.

Theorem 1: Consider the train with n carriages, and M is unknown but constant. Let $u = \Lambda F$. If the following control scheme is implemented,

$$u = \hat{M}(\ddot{x}^* - \beta\dot{e}) - k_0 s + F_r \tag{11a}$$

with

$$F_r = -\frac{\hat{b}\Phi^2 s}{\Phi|s| + \varepsilon_0\exp(-ct)} \tag{11b}$$

$$\begin{aligned} \dot{\hat{M}} &= -\lambda_m s(\ddot{x}^* - \beta\dot{e}) \\ \dot{\hat{b}} &= \sigma\frac{\Phi^2|s|^2}{\Phi|s| + \varepsilon_0\exp(-ct)} \end{aligned} \tag{11c}$$

where $k_0 > 0$ is a free control parameter; ε_0, and c are positive constants chosen by designer; $\hat{M}$ and $\hat{b}$ are the estimated value of M and b, respectively; $\lambda_m > 0$; $\sigma > 0$ is a small positive constant which can adjust the change rate of $\hat{b}$. Then asymptotic speed and position tracking is achieved in that $e \to 0$, $\dot{e} \to 0$ as $t \to \infty$.

Proof:

Based on Eqs. (8) and (11a), we can get

$$M\dot{s} = -k_0 s + \tilde{M}(\ddot{x}^* - \beta\dot{e}) + F_r + F_d \tag{12}$$

Consider the Lyapunov function candidate

$$V=\frac{1}{2}Ms^2+\frac{\tilde{M}^2}{2\lambda_m}+\frac{1}{2}\frac{(b-\hat{b})^2}{\sigma} \tag{13}$$

where

$$\tilde{M}=\hat{M}-M$$

with the control algorithms given in Eqs. (11a)-(11c), it follows that

$$\begin{aligned}\dot{V}&=sM\dot{s}+\tilde{M}\frac{\dot{\hat{M}}}{\lambda_m}+(b-\hat{b})(\frac{-\dot{\hat{b}}}{\sigma})\\&=-k_0s^2+s(F_r+F_d)+(b-\hat{b})(\frac{-\dot{\hat{b}}}{\sigma})\\&\leqslant -k_0s^2-\frac{\hat{b}\Phi^2|s|^2}{\Phi|s|+\varepsilon_0\exp(-ct)}+b\Phi|s|+\frac{1}{\sigma}(b-\hat{b})(-\dot{\hat{b}})\\&=-k_0s^2+\frac{b\Phi|s|\varepsilon_0\exp(-ct)}{\Phi|s|+\varepsilon_0\exp(-ct)}\\&\leqslant -k_0s^2+b\varepsilon_0\exp(-ct)\end{aligned} \tag{14}$$

where the two inequations $\frac{\Phi|s|}{\Phi|s|+\varepsilon_0 e^{-ct}}\leqslant 1$, and $|F_d|\leqslant b\Phi$, ($\forall\Phi\geq 0$) are employed. From Eq. (14) we get $V\in\ell_\infty$, implying that $s\in\ell_\infty$, $\hat{M}\in\ell_\infty$, $\hat{a}_0\in\ell_\infty$, $\hat{a}_1\in\ell_\infty$, $\hat{a}_2\in\ell_\infty$ and $\hat{b}\in\ell_\infty$, which ensure that $\Phi\in\ell_\infty$, $\dot{\hat{b}}\in\ell_\infty$, thus $u\in\ell_\infty$. Furthermore, from (12) we have $\dot{s}\in\ell_\infty$, i.e., s is uniformly continuous. Also since $\int_0^t s^2dt\leq V(0)<\infty$, it is already established that $s\in\ell_2\cap\ell_\infty$, then by Barbalat Lemma, it is concluded that $\lim_{t\to\infty}s=0$, therefore $\dot{e}\to 0$, $e\to 0$ as $t\to\infty$ by the definition of s.

Remark 4 It is interesting to note that the proposed control strategy is able to achieve position and speed tracking based upon x_1 and $\dot{x}_1$, without the need for x_i, and $\dot{x}_i$ ($i=2,3,\cdots,n$). Namely, it requires much less number of sensors for speed and position measurement as compared with those methods that involve x_i and $\dot{x}_i$ ($i=1,2,\cdots,n$).

Remark 5 It is seen that the developed control scheme can be implemented without the need for precise information on M, a_0, a_1, a_2, and the bound coefficient b.

The following result presents a solution that further simplifies the control scheme in that only one lumped control parameter estimation is needed. To this end, we combine the last two terms in (8) as

$$L_d(\cdot)=-M(\ddot{x}^*-\beta\dot{e})+F_d(\cdot)$$

Assume that $\ddot{x}^*$ and $\dot{x}^*$ are bounded, which always holds in practice, then we can shown that

$$|L_d|\leqslant l_1+l_2|\dot{x}|+l_3|\dot{x}|^2\leqslant l\Phi$$

where Φ is defined the same as in Eq. (10) and l_1, l_2 and l_3 are some non-negative constants, and $l=\max\{l_1,\ l_2,\ l_3\}$. Note that l is difficult to obtain precisely as with the case of b, therefore, an adaptive algorithm is derived to estimate such parameter on-line, as presented in the following theorem.

Theorem 2 Consider the train with n carriages. If the following control scheme is implemented,

$$u=-k_0s+F_r \tag{15a}$$

with

$$F_r=-\frac{\hat{l}\Phi^2 s}{\Phi|s|+\varepsilon_0\exp(-ct)} \tag{15b}$$

$$\dot{\hat{l}}=\sigma\frac{\Phi^2|s|^2}{\Phi|s|+\varepsilon_0\exp(-ct)} \tag{15c}$$

where k_0, σ ε_0, c are control parameters defined as before, $\hat{l}$ is the estimated value of l. Then asymptotic speed and position tracking is achieved in that $e\to 0$, $\dot{e}\to 0$ as $t\to\infty$.

Proof:

From Eqs. (8) and (15a), we have

$$M\dot{s}=-k_0s+F_r+L_d \tag{16}$$

Consider the Lyapunov function candidate

$$V=\frac{1}{2}Ms^2+\frac{1}{2}\frac{(l-\hat{l})^2}{\sigma} \tag{17}$$

Its deriva tive with respect to time becomes

$$\begin{aligned}\dot{V}&=sM\dot{s}+(l-\hat{l})(\frac{-\dot{\hat{l}}}{\sigma})\\&=-k_0s^2+s(F_r+L_d)+(l-\hat{l})(\frac{-\dot{\hat{l}}}{\sigma})\\&\leqslant -k_0s^2+sF_r+l\Phi|s|+(l-\hat{l})(\frac{-\dot{\hat{l}}}{\sigma})\\&=-k_0s^2+\frac{l\Phi|s|\varepsilon_0\exp(-ct)}{\Phi|s|+\varepsilon_0\exp(-ct)}\\&\leqslant -k_0s^2+l\varepsilon_0\exp(-ct)\end{aligned} \tag{18}$$

The result is established using the same argument as in the proof of Theorem 1.

Remark 6 It turns out that the derived control scheme can be easily set up and implemented because such control scheme only involves on-line estimation of one control design parameter, as a result, much fewer onboard computing resources are needed in the presented control scheme as compared with most existing methods.

3.3 Optimal Power/Brake Distribution

One needs to determine F_i, ($i=1,2,\cdots,n$) from $u=\Lambda F$ and Eqs. (11) and (15). To achieve optimal distribution, the following optimal problem is to be solved,

$$\text{Minimize: } J=\frac{1}{2}F^TPF \tag{19}$$

$$\text{Subject to: } \Lambda F=u \tag{20}$$

Using Lagrangian multiplier method, F can be obtained

$$F=P^{-1}\Lambda^T\left[\Lambda P^{-1}\Lambda^T\right]^{-1}u \tag{21}$$

Where P is a positive definite matrix. See [12] for proof. Note that F as determined by (21) makes the energy function (19) minimized. Such F represents the total (combined) driving/braking force contributed by each power engine and braking system. If the vehicle is a locomotive, it provides both traction force (F_P) and braking force (F_B). If the vehicle is a carriage, it provides braking force only. For a train consisting of n vehicles with q locomotives

and p carriages ($n=p+q$), the driving/braking force obtained by (21) should also satisfy the following:

- For locomotives,

$$F_P^i=\varphi F_i \quad \left(i=M_1, M_2, ..., M_q\right) \tag{22a}$$

$$F_B^i=\gamma F_i \quad \left(i=M_1, M_2, ..., M_q\right) \tag{22b}$$

- For carriages,

$$F_B^j=\gamma F_j, \quad \left(j=T_1, T_2, ..., T_p\right) \tag{23}$$

where the traction or braking mode is determined by the sign of u through

$$\varphi=\frac{1+sign(u)}{2} \text{ and } \gamma=\frac{1-sign(u)}{2}.$$

As can be verified, if $u\geqslant 0$ one has $\varphi=1$ and $\gamma=0$, leading to $F_P^i=F_i$ and $F_B^j=0$, implying that traction (power) is required from the engine of the locomotive and no braking force is necessary at this time; If $u<0$, then one has $\varphi=0$ and $\gamma=1$, resulting in $F_P^i=0$, $F_B^i=F_i$ and $F_B^j=F_j$, implying that no motoring force is needed and that both the locomotive and the carriage are required to provide braking forces at this time. Therefore, the practical situation is well reflected in the setting as given in (22~23). Fig. 3 depicts the block diagram of the unified adaptive traction and braking control scheme.

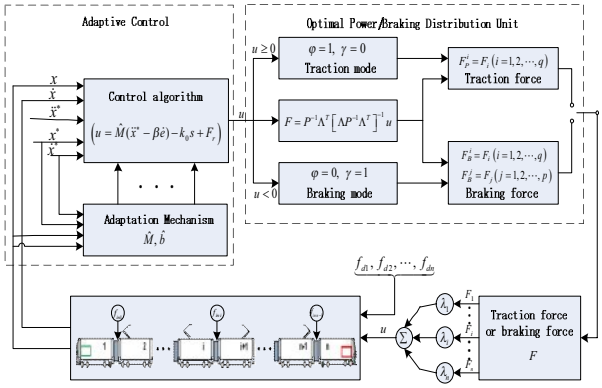

Fig. 3 Block diagram of the unified adaptive traction and braking control scheme

4 SIMULATION STUDIES

Here, we present the simulation results of control algorithms (11a)-(11c). To verify the effectiveness of the proposed control scheme, a series of simulation studies based on a train similar to CRH2-A with eight vehicles (i.e., 4 locomotives and 4 carriages as illustrated in Fig. 4) are conducted and ranked from headstock to rear using the numbers 1 to 8. To account for the uncertain mass of each vehicles as mentioned in early sections, the total mass for the train (8 vehicles) used for simulation is set as $M=(345+\Delta M)(ton)$, distributed among the train equally, where ΔM denotes the uncertain portion of the mass. Note that both M and ΔM are not needed in control design. The resistance coefficients simulated could be any value of the range as follows respectively,

$$a_0\in[50, 85],\ a_1\in[30, 100],\ a_2\in[0.1, 6.5]$$

which covers a wide class of trains including CRH and SS1 series [16]. The additional resistance for each vehicle is of the form

$$f_{ri}=338.445\sin(0.2t)[U(t-4)-U(t-12)]\ (N),$$

$$f_{ci}=338.445+338.445\sin(0.5t)\ (N),$$

$$f_{ti}=676.89\sin(0.1t)\sin(0.2t)\ (N),\quad i=(1,\ 2,\ \cdots,\ 8).$$

For simulation purpose, we consider the case that the spring deformation of the coupler varies according to the following relations,

$$\Delta x_{d1}=\Delta x_{d3}=\Delta x_{d4}=0.1\sin t\ (mm),$$

$$\Delta x_{d6}=\Delta x_{d7}=0.15\cos t\ (mm),$$

$$\Delta x_{d2}=\Delta x_{d5}=0.1\cos t\ (mm).$$

The travel distance tested in our simulation is $37.087km$. The power/braking effort distribution for each vehicle is as follows:

$\lambda_i=1\ (i=2,3,6,7)$ (locomotives: M1, M2, M3,M4)

$\lambda_j=1\ (j=1,4,5,8)$ (carriages: T1, T2,T3,T4)

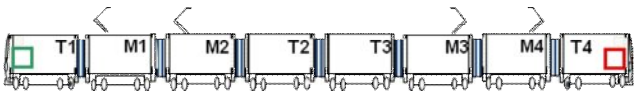

Fig. 4 CRH2-A with 4 locomotives (M) and 4 carriages (T)

The control parameters are chosen arbitrarily as $\beta=2.5$, $k_0=1\times10^7$, $\varepsilon_0=0.1$, $c=0.01$, $\sigma=0.5$.

The goal is to make the actual velocity v and position s track the desired velocity v^* and desired position s^* with high precision.

The actual position and velocity tracking process (top) and the tracking error (bottom) under control scheme (11) is depicted in Fig. 5. One can observe good tracking control performance.

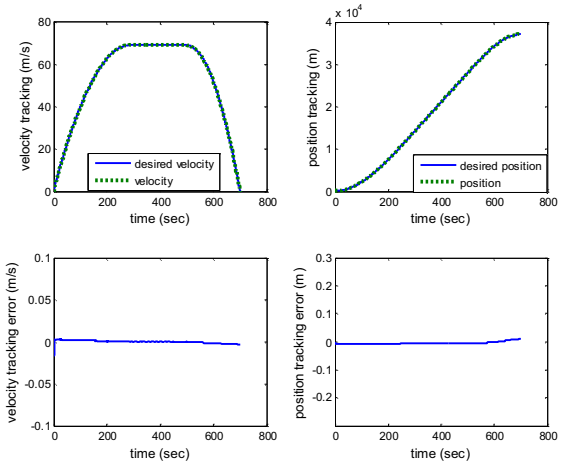

Fig. 5 Velocity and position tracking process and errors under control scheme (11)

The real control forces contributed by each vehicle under control scheme (11) is shown in Fig. 6 and Fig. 7, where the traction forces are presented in Fig. 6 and the barking forces

are shown in Fig. 7. It can be observed from these figures that the locomotive vehicles (with motoring and braking capabilities) indeed provide the traction forces during traction phase and the braking forces during braking phase (Fig. 6), whereas the carriage vehicles (without motoring capabilities) only provide the braking forces during braking phase (Fig. 7), which agrees with our theoretical prediction.

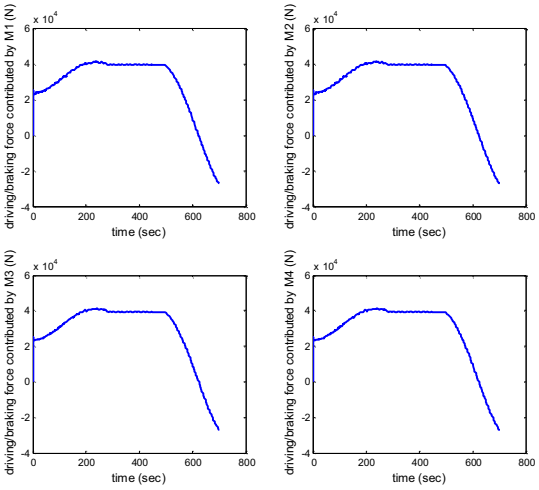

Fig. 6 Driving/Braking force contributed by locomotives

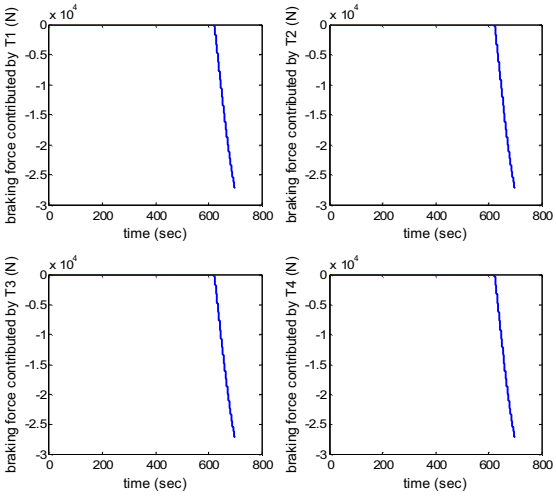

Fig. 7 Braking force contributed by carriages

As theoretically predicted, the robust adaptive control scheme is able to achieve fairly good control performance without using any information on system parameters, or the upper bound coefficient of $|F_d|$.

5 CONCLUSIONS

An improved multiple point-mass model for high speed train consisting of n vehicles (locomotives and carriages) is presented in this paper. Robust and adaptive control with optimal power/brake distribution is proposed to achieve high precision position and speed tracking control in the presence of uncertain system parameters and interactive in-train impacts. The attraction feature of the proposed control lies in its simplicity in design and implementation, which makes it possible to continuously maintain high precision tracking control of the train during the entire operation without requirement of re-design or re-programming of the controller under widely varying operation conditions.

REFERENCE

[1] Sinha, P. K.. Electromagnetic Suspension Dynamics and Control, vol. 30, IEE Control Engineering Series,Peter Peregrinus, London, 1987.

[2] P. Howlett. Optimal strategies for the control of a train. Automatica, Apr. 1996, 32(4): 519–532,.

[3] Ciann-Dong Yang and Yun-Ping Sun. Auto-Pilot System of High Speed Rail. Proceedings of Joint Meeting of the World Multiconference on Systemic, Cybernetics and Informatics (SCI'98) and the 4"Jnternational Conference on Information Systems Analysis and Synthesis (ISAS'98), 1998,:4.

[4] Gorgon, S. P. and Lehrer, D. G.. Coordinated Train Control and Energy Management Control Strategies. Proceedings of the 1998 ASMELIEEE Joint Railroad Conference, Philadelphia, USA, 1998: 165-176.

[5] R. Liu and I. M. Golovitcher. Energy-efficient operation of rail vehicles. Transport. Res., 2003, 37: 917-932.

[6] C. Yang and Y. Sun. Robust cruise control of high speed train with hardening/softening nonlinear coupler. In Proc. Amer. Control Conf., 1999: 2200-2204.

[7] C. Yang and Y. Sun. Mixed H_2 / H_∞ cruise controller design for high speed train. Int. J. Control, 2001, 74(9): 905–920.

[8] A. Astolfi and L. Menini, "Input/output decoupling problem for high speed trains," in Proc. Amer. Control Conf., 2002, . 549–554.

[9] X. Zhuan and Xiaohua Xia. Optimal Scheduling and Control of Heavy Trains Equipped With Electronically Controlled Pneumatic Braking Systems. IEEE Transactions on Control Systems Technology, 2007, 15(6): 1159-1166.

[10] M. Chou, X. Xia, and C. Kayser. Modelling and Model validation of heavy-haul trains equipped with electronically controlled pneumatic brake systems. Control Engineering Practice, 2007, 15(4): 501-509.

[11] M. Chou and X. Xia. Optimal Cruise Control of Heavy Haul Train Equipped with Electronic Controlled Pneumatic Brake Systems. Presented at the 16th IFAC World Congress, Prague, Czech Republic, 2005.

[12] Y. D. Song, J. N. Anderson, and H. Y. Lai. Robust Control of Multi-Robot Systems: The Generalized Energy Accumulation Approach. International Journal of Robust and Nonlinear Control, 1994, 4: 673-696.

[13] Wenying Huang, Ningqing Yang, Min Huang. Ponderation on Railway Train Basic Resistance. China Railway Science, 2000, 21(3): 44-57.

[14] Weidong Wang, Qiyong He. Dynamic problems in high-speed train systems. Mechanical Progress, 1995, 25(1): 134-143.

[15] Hongqi Tian. Study on the Characteristics of Train Air Resistance under Wind Environment. China Railway Science, 2008, 29(5): 108-112.

[16] Zhong Rao. Train traction calculation. Beijing: China Railway Press，2005.